14th International Symposium on Turbulence and Shear Flow Phenomena (TSFP14)
Heidelberg, Germany, July 28–31, 2026

STRAIFIED MIXING LAYERS EXPERIMENTS IN SODIUM AND WATER

Ralf Kapulla
PSI Center for Nuclear Engineering and Sciences
5232 Villigen PSI, Switzerland
ralf.kapulla@psi.ch

Ulrich Doll
Department of Mechanical and Production Engineering
Aarhus University, 8200 Aarhus N, Denmark
ud@mpe.au.dk

Abstract

LIQUID SODIUM SHEAR LAYER experiments were designed to analyse the effects of *stable* thermal stratification at very low Prandtl numbers ($Pr \leq 10^{-2}$) on turbulent exchange mechanisms with the Richardson number as the parameter. The results are compared with measurements in a geometrically and hydraulically similar water test section with $Pr \approx 6$. Special attention is drawn for the present publication to the fact, that for stronger stratifications in liquid sodium, the fast spreading rate of the temperature field causes a pronounced acceleration of the upper, slower part of the flow, *outside the* ***core*** *of the hydraulic mixing layer*, as well as a deceleration in the middle of the mixing layer. The experimental and theoretical results indicate that these effects observed in liquid sodium shear layers are attributable to the repercussions of temperature on the velocity field. This assertion will be elaborated upon and is the focus of this article.

Introduction

THE PLANE MIXING LAYER that forms at the interface between two co- or counter flowing uniform streams of different velocity is one of the canonical flows that have been extensively studied. Using water (Kapulla *et al.* (2022)) or gases (Brown & Roshko (1974)) for the respective stratified shear- or mixing-layer experiments is commonplace. Corresponding liquid sodium experiments, however, are rare and difficult to find in the literature (Shams *et al.* (2020)). The Reynolds or Prandtl number analogy for turbulent flows suggests that, for $Pr \approx 1$, there is a similarity between heat and momentum transport with the consequences that the velocity and temperature profiles have the same or a similar shape. This condition ($Pr \approx 1$) holds true for most of the gases and, to a certain extent, also for water ($Pr \approx 5$ at $30°C$), but not for liquid sodium ($Pr \approx 0.007$ at $250°C$). Therefore, experiments involving a shear layer of liquid sodium provide an interesting benchmark for determining the extent to which physical models and concepts developed for water and air can be also applied. To the best of the author's knowledge, this is the *only* experiment ever conducted in this realm – in conjunction with a geometrically and hydraulically scaled water test facility.

Liquid Sodium Facility

THE LIQUID SODIUM EXPERIMENTS were conducted in the specially designed stainless steel mixing layer test section NAMIX, Figure 1.
A stable two-layer configuration is considered, in which the bottom and top legs of the liquid sodium are conditioned separately. Different shear conditions are achieved by adjusting the mean velocity difference $\Delta\overline{u}$ between the two legs with the bottom leg being faster ($\overline{u}_1 > \overline{u}_2$). The stable stratification strength is adjusted with the mean temperature difference $\Delta\overline{T} = \overline{T}_2 - \overline{T}_1$ between the two legs, with $\overline{T}_2 > \overline{T}_1$. The facility can be tilted clockwise (↷) or anti-clockwise (↶) to adjust the position of the mixing layer relative to the acceleration of gravity.

Six measurement positions are provided at the non-dimensional downstream distances $x/l_g = 0.84$, 2.84, 4.84, 6.84, 8.84, 10.84 with $l_g = 100\ mm$. The parameter l_g depicts the distance between the last two grids in the water and liquid sodium facility. However, we will only use some of these downstream results in this article. Miniature permanent-magnet probes (PMV probes, details provided in Kapulla *et al.* (2000)) can be vertically traversed at these positions to measure both the velocity in x-direction as well as the temperature. The upper and lower walls of the facility exhibit a slight inclination ($\triangleleft$)[1], a design feature intended to compensate for the growth of the boundary layers for the velocity ratio $r = \overline{u}_2/\overline{u}_1 = 0.6$ these experiments were designed for. In the absence of this inclination, the core flow would accelerate with downstream distance.

Measurement Techniques

IN LIQUID SODIUM streamwise velocities **and** temperatures are measured by means of in-house build temperature and thermocouple inertia compensated PMV probes. The PMV probe is essentially based on Faraday's law of

[1]The opening angle was set *differently* relative to the centreline of the test section, which is defined as the horizontal extension of the splitter plate. This is because lower velocities were consistently set for the upper leg than for the lower leg. At lower velocities, a greater increase in the boundary layer is expected (Schlichting & Gersten (2017)). This was taken into account. Consequently, the corresponding opening angle of the facility in the upper leg was slightly larger.

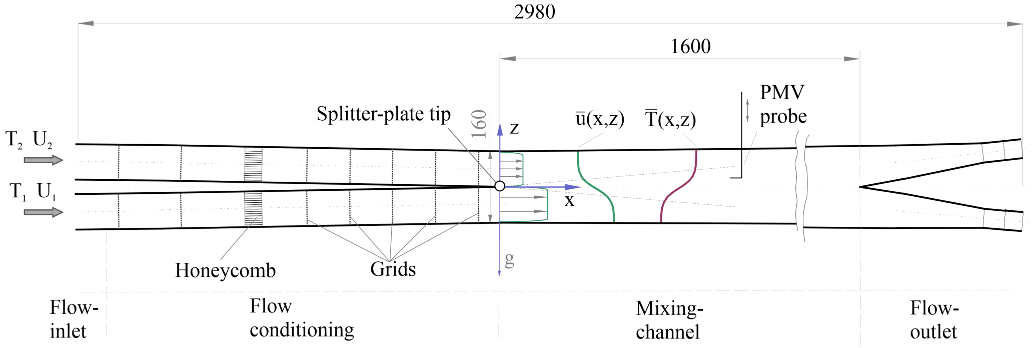

Figure 1. Schematic of the liquid sodium test facility NAMIX.

induction and results from a generalised form of Ohm's law which can be translated into the Poisson equation for the velocity proportional potential difference Φ from which the final velocity signal can be deduced. Further details, more theoretical background, the calibration procedure and the signal evaluation can be found in (Kapulla *et al.* (2000)).

In water, the velocity measurements were performed by means of a 2D laser Doppler anemometer, see (Albrecht *et al.* (2003)). A hot wire anemometer (HWA) probe (Bruun (1995)) was used to undertake simultaneous temperature measurements, with the probe positioned at a distance of 1 mm downstream from the LDA measurement volume. This precautionary measure was implemented to circumvent any potential disturbances to velocity measurements. Both the LDA measurement volume and the HWA were simultaneously vertically traversed.

Results and Discussion

The emphasis of this study is on the presentation of the results of the mixing layer for stable stratification in the sodium experiments, in conjunction with the results obtained in a geometrically and hydraulically similar water test section.

The free stream turbulence affects both the development of the mixing layer and the persistence of the vortical structures, see Chandrsuda *et al.* (1978). Thus, the grid Reynolds numbers

$$Re_{d,1(2)} = \frac{\overline{u}_{1(2)} \cdot d}{\nu} \tag{1}$$

in both streams, calculated with the wire gauge d of the last grid before the end of the splitter plate and the time averaged mean velocities $\overline{u}_{1(2)}$ must be the same in the water (w) and liquid sodium (s) facilities to obtain similar entrance hydraulic conditions. For water at $30°C$ and liquid sodium at $250°C$, the ratio of the kinematic viscosities $\nu_w : \nu_s$ is almost $2:1$. Therefore, with velocity ratios $\overline{u}_w : \overline{u}_s = 2:1$ and geometrically similar test sections with the same grid configuration (i.e. the same grid spacing $l_g = 100\,mm$, wire gauges $d_w = d_s = 0.6\,mm$ and distance between the wires $l_w = l_s = 2.0\,mm$), the test facilities are also physically similar with respect to flow conditioning, as quantified by eq. (1). All the grid Reynolds numbers are supercritical, i.e. above a numerical value of 60 (Groth & Johansson (1988)).

Observations

We first provide some observations based on the normalized velocity and temperature measurements presented in Figures 2 and 3, before we delve into the corresponding physical explanation attempts.

If we begin with the results from the water test section (Figure 2, bottom row), we can see that (a) the hydraulic mixing layer expands downstream in the vertical direction and (b) the experimental results can be well approximated by *tanh* profiles according:

$$\overline{u}(x,z) = \overline{u}_m + \frac{\Delta\overline{u}}{2} tanh\left(\frac{z - z_{ct,u}}{\delta_u/2}\right) \tag{2}$$

where $\overline{u}_m = (\overline{u}_1 + \overline{u}_2)/2$ denotes a mean velocity, z_{ct} the centre of the profile and δ_u the thickness of the hydraulic mixing layer.

Similar observations can also be made regarding the development of the thermal mixing layer which is approximated with:

$$\overline{T}(x,z) = \overline{T}_m + \frac{\Delta\overline{T}}{2} tanh\left(\frac{z - z_{ct,T}}{\delta_T/2}\right) \tag{3}$$

This would also make it possible to represent both the hydraulic and thermal mixing layers in self-similar coordinates (Yarin (2012)), although this will not be discussed further in this article. Even though the expansion rates for the hydraulic and thermal mixed layers are not identical, there is nevertheless a coupling, as would be expected for $Pr \approx 6$. The thermal mixing layer grows slightly faster overall.

The picture is quite different when it comes to the corresponding results in liquid sodium, Figure 2, top row. Just beyond the tip of the splitter plate ($x/l_g = 0.84$), we find a

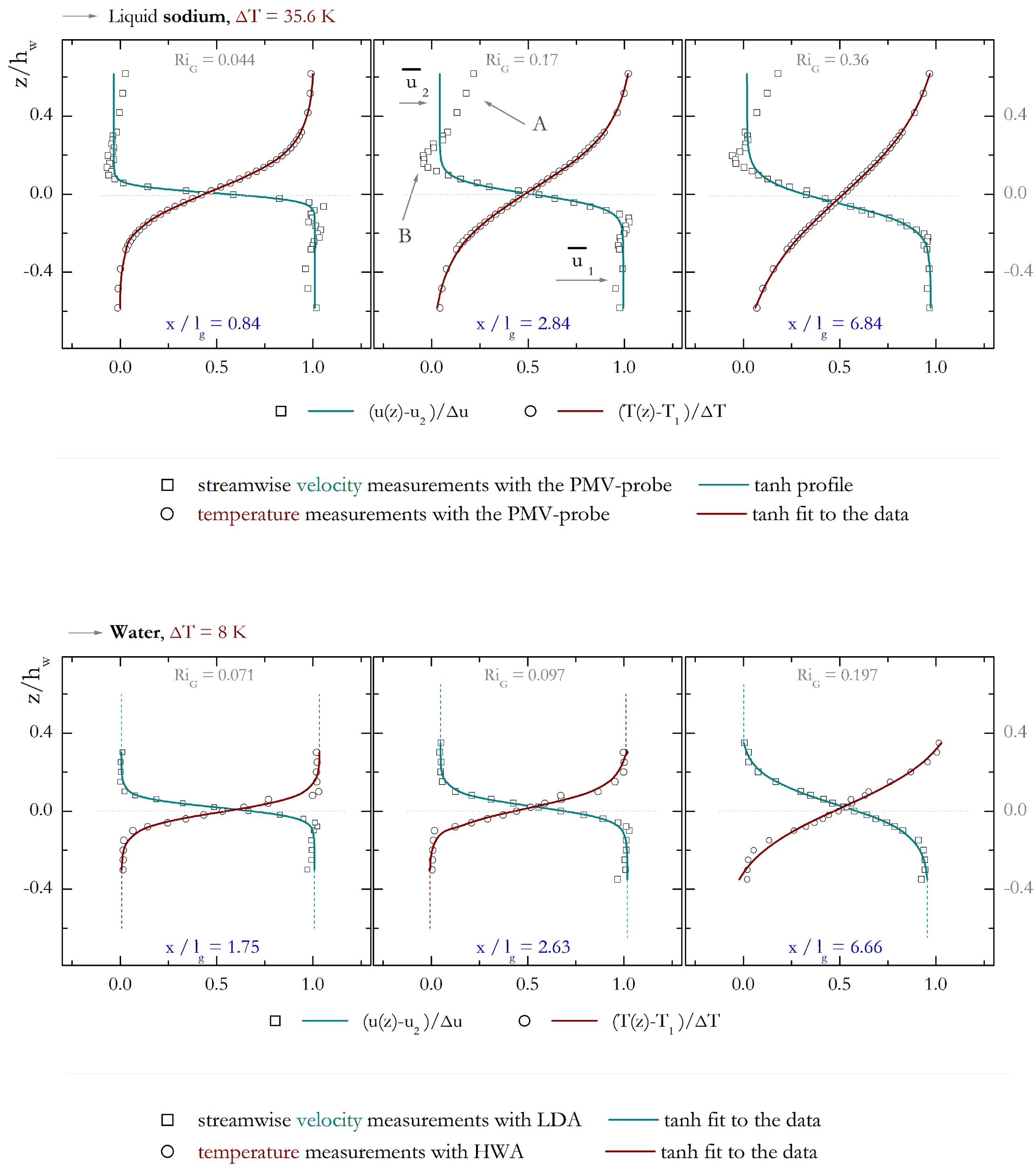

Figure 2. Development of the normalized mean velocity (□) and temperature (○) profiles in liquid sodium (top row) and water (bottom row) for three downstream distances. The approximations for the velocity profiles in liquid sodium are given to guide the eye.

velocity profile that is quite comparable to those in water. Further downstream, however, the upper (slower) stream accelerates (Mark A), and slightly above the centre of the test section, there is a corresponding deceleration (Mark B). Neither of these effects can be observed in the experiments conducted in water. The development of the thermal layer is almost completely decoupled from the hydraulic mixing layer and, as a result, grows much faster; this is particularly evident when we compare it with the measurements taken in water.

In order to comprehend the phenomena occurring in liquid sodium, it is necessary to first direct attention to Figure 3. In the top row, the temperature difference between the lower and upper streams was systematically varied for a horizontally oriented test section. The bottom row presents results obtained for constant thermal stratification but different angles of inclination of the test section. We can now make the following observations:

1. For the horizontally aligned test section, we monitor an acceleration in the upper leg of the flow. This acceleration increased with increasing temperature (ΔT) stratification strengths; effect-I (e-I).

2. Again for the horizontally aligned test section, we measure the highest velocity deficit almost in the middle of the facility ($z/h_w \approx 0$) which increases

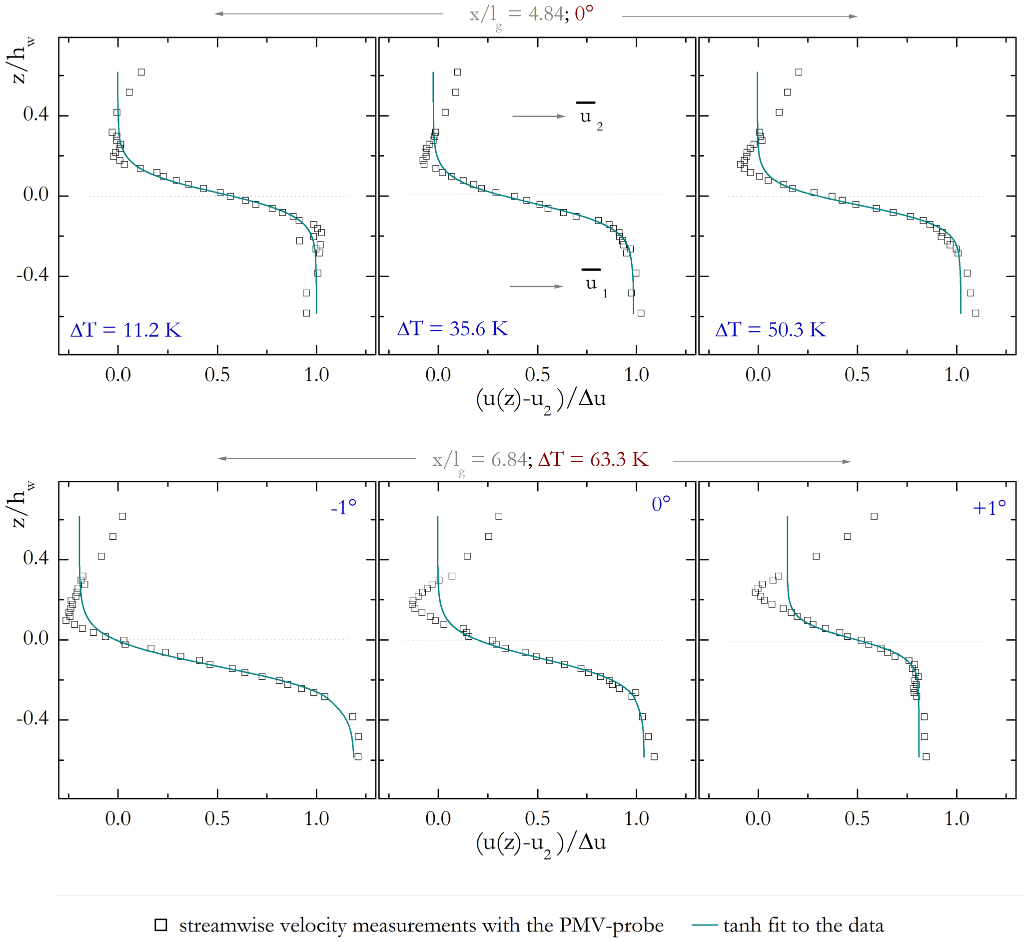

Figure 3. Streamwise ($\rightarrow$, u_x) velocity profile *acceleration* in the upper, slower stream as a function of the temperature stratification strength (ΔT) for a horizontally aligned test section (0°) measured (□) at identical downstream distances ($x/l_g = 4.84$) – top row. Acceleration of the velocity profiles in the upper part of the flow as a function of the test section inclination ($-1°$ ↶, $\rightarrow 0° \leftarrow$, $+1°$ ↷), for a single strong temperature stratification ($\Delta T = 63$ K) – bottom row.

with increasing stratification strengths – when compared to a *tanh*-profile which is presented to guide the eye and to demonstrate the deviation from a classical self-preserving mixing layer; effect-II (e-II).

3. Interestingly enough, both e-I and e-II can be modulated by very (!) weakly inclining the facility ($\pm 1°$); Figure 2, bottom row, for a fixed stratification strength of $\Delta T = 63.4$ K.

Physical background

Using the time averaged, two dimensional Navier-Stokes equations (Rodi (1984)), it is shown in (Kapulla (1999)) that one can derive, with corresponding order of magnitude assumptions and simplifications, the velocity behaviour in the upper part (↑, index 2) of the liquid sodium facility:

$$\frac{\partial}{\partial x}\frac{\overline{u}_2{}^2}{2} = \frac{\partial}{\partial x}\frac{\overline{u}_1{}^2}{2} + \beta \cdot \Delta\overline{T} g\,(m_T + tan(\varepsilon)) \qquad (4)$$

where β depicts the thermal expansion coefficient of liquid sodium, $\Delta\overline{T}$ the temperature difference across the mixing layer, m_T the slope of the line connecting the centres of the temperature profiles ($z_{cT} = z_{T0} + m_T \cdot x$), g the acceleration of gravity and ε the inclination angle of the facility, see also Figure 4. Experimental values for m_T can be found in Table 1.

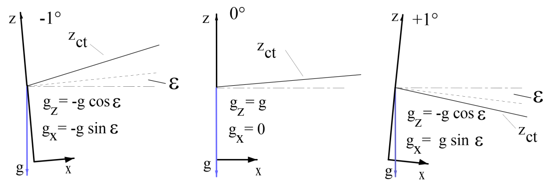

Figure 4. Generic relative position of the coordinate system inside the test section with respect to the direction of the gravitational force for different test section inclinations.

This now means that, for $m_T + tan\varepsilon > 0$, the fluid outside of the hydraulic mixing layer in the upper, slower, warmer part ($\overline{u}_2$) will be accelerated compared to the colder stream at the bottom. This acceleration is directly proportional to the stratification strength, ΔT, and $m_T + tan\varepsilon$ which characterises the inclination of the test section with respect to the direction of the gravitational force. The dependence on ΔT is shown in the top row (inclination angle $\varepsilon = 0°$ was kept constant, ΔT var-

Table 1. Experimentally determined slopes, m_T, for the linear fit to the thermal mixing layer centres for different test section inclinations; $\Delta T = 63.3$ °C

	$\varepsilon = -1°$	$\varepsilon = 0°$	$\varepsilon = +1°$
m_T	$11.8 \cdot 10^{-3}$	$5.0 \cdot 10^{-3}$	$-17.0 \cdot 10^{-3}$

ied) and the dependence on $m_T + tan\varepsilon$ ($\Delta T = 63.3$ K kept constant, inclination ε varied) in the bottom row of Figure 3.

In a similar manner, an equation for an almost horizontal stream line in the middle of the mixing layer ($z/h_w \approx 0$) can be derived:

$$\overline{u}^2 \approx \overline{u}_o^2 - \beta \cdot g \frac{\Delta \overline{T}}{2} ln(2)(\delta_T - \delta_{T0}) \quad (5)$$

where the index 0 denotes initial conditions at the stream line origin, $\overline{u}$ the mean velocity along the stream line and δ_T (eq. (3)) the thermal mixing layer thickness. Note that this velocity deficit is independent of the test section inclination ε. According to eq. (5), the velocity deficit in the middle of the facility is only proportional to the temperature difference $\Delta \overline{T}$ and the thermal mixing layer thickness δ_T, see also Figure 3.

These two effects discussed *separately*, i.e. the acceleration of the slower, upper leg and the velocity deficit in the middle of the test section, are generally superimposed, and the measured velocity profiles in sodium show a combination and interdependence of both. For the test section inclined clockwise, with an inclination of $\varepsilon = +1°$, the fluid in the warmer top leg is accelerated, while on the colder, slower side decelerated. This results in a decrease in the velocity difference, $\Delta \overline{u}$, across the mixing layer, see Figure 2, bottom row, right. Thus, the normalised velocity in the colder, faster leg is below one. For this alignment of the facility the acceleration in the upper leg (e-I) and the deceleration in the middle part (e-II) are most pronounced. The faster spread of the thermal mixing layer, as well as the higher temperature gradients in sodium compared to the water tests, mean that the velocity deficit and, in consequence, the redistributed fluid towards the upper stream — resulting in an acceleration — cannot be observed in the corresponding water experiments.

Summary

In this study, geometrically and hydraulically similar mixing layers in water and liquid sodium were compared against each other.

Both experimental and theoretical evidence suggests that the velocity field of stably stratified shear layers in *liquid sodium* may deviate significantly from self-preserving behaviour and depend both on the stratification strength and the details of the inclination of the test section. An acceleration in the top part of the flow and a velocity deficit in the middle of the hydraulic mixing layer were observed, and attempts were made to explain them.

To the best of the author's knowledge, this is the only experiment for stratified shear flows ever conducted in the realm of liquid sodium – in conjunction with a geometrically and hydraulically similar water test facility – to present both results face-to-face.

References

Albrecht, H.E., Borys, M., Damaschke, N. & Tropea, C. 2003 *Laser Doppler and Phase Doppler Measurement Techniques*. Springer Verlag.

Brown, G. L. & Roshko, A. 1974 On density effects and large structure in turbulent mixing layers. *J. Fluid Mech.* **64**, pp. 775–816.

Bruun, H. H. 1995 *Hot-wire Anemometry*. Oxford University Press.

Chandrsuda, C., Mehta, R. D., Weir, A. D. & Bradshaw, P. 1978 Effect of free-stream trubulence on large structure in turbulent mixing layers. *J. Fluid Mech.* **85**, pp. 693–704.

Groth, Johan & Johansson, Arne V. 1988 Turbulence reduction by screens. *Journal of Fluid Mechanics* **197**, 139–155.

Kapulla, R. 1999 *Experimentelle Untersuchung von thermisch stratifizierten und unstratifizierten Mischungsschichten in Natrium und Wasser*. PhD Thesis, ETH Zürich, Nr. 13430.

Kapulla, R., Doll, U., Kirkby, E. & Paranjape, S. 2022 Growth laws and self-similarity in the confined mixing zone of unstratified and strongly stably stratified isokinetic mixing-layers past a splitter plate. *Physics of Fluids* **34** (3), 035129.

Kapulla, R., Sigg, B., Horanyi, S. & Hudina, S. 2000 Local velocity measurements in a thermally-stratified sodium mixing layer using a permanent-magnet probe. *Experimental Thermal and Fluid Science* **20** (3-4), 115 – 136.

Rodi, W. 1984 *Turbulence models and their application in hydraulics*. IAHR, State-of-the-Art-paper, Presented by the IAHR-Section on Fundametals of Division II,: Experimental and mathematical Fluid Dynamics.

Schlichting, H. & Gersten, K. 2017 *Boundary-Layer Theory*. Springer Berlin, Heidelberg.

Shams, A., Roelofs, F., Tiselj, I., Oder, J., Bartosiewicz, Y., Duponcheel, M., Niceno, B., Guo, W., Stalio, E., Angeli, D., Fregni, A., Buckingham, S., Koloszar, L.K., Villa Ortiz, A., Planquart, P., Narayanan, C., Lakehal, D., van Tichelen, K., Jäger, W. & Schaub, T. 2020 A collaborative effort towards the accurate prediction of turbulent flow and heat transfer in low-prandtl number fluids. *Nuclear Engineering and Design* **366**, 110750.

Yarin, L.P. 2012 *The Pi-Theorem - Applications to Fluid Mechanics and Heat and Mass Transfer*. Springer Berlin, Heidelberg.